Influence of added mass on anomalous high rise velocity of light particles in cellular flow field: A note on the paper by Maxey (1987)

Cristian Marchioli, Marco Fantoni, and Alfredo Soldati[a)]
Centro Interdipartimentale di Fluidodinamica e Idraulica, Dipartimento di Energetica e Macchine, Università degli Studi di Udine, Via delle Scienze 208, Udine 33100, Italy

(Received 10 October 2006; accepted 31 May 2007; published online 7 September 2007)

In this Brief Communication, we examine in detail the motion of light particles—or dense gas bubbles—rising under gravity in a cellular flow. We follow the methodology of Maxey [Phys. Fluids **30**, 1915 (1987)], and we examine a range of parameters not fully discussed in the past, corresponding to particles lighter and yet more inertial than the surrounding fluid if the added mass effect is considered. We observe a nonmonotonic behavior of the particle rise velocity, which exhibits a maximum for density of the particles only slightly smaller than the density of the fluid. The maximum value of the average rise velocity corresponding to the "optimum" density is several times (more than 40) higher than those obtained for small density changes around the optimum. The occurrence of this maximum is due to the combined effects of particle inertia and fluid added mass, which segregate the rising particles into specific, fast pathlines where the local fluid velocity adds to the particle gravitational velocity. A plot covering particle rise velocity for this range—not covered by the analysis of Maxey—is provided. © *2007 American Institute of Physics*.
[DOI: 10.1063/1.2759528]

A comprehensive study on the influence of turbulence on the effective particle settling velocity was performed by Maxey.[1] In that work, an analytic cellular flow field was taken to mimic a simplified turbulent flow and the effect of different particle parameters was investigated using Lagrangian tracking. Results are well known and widely cited: Particle behavior was found to depend on particle-to-fluid time scale and on particle-to-fluid density ratio. The attention was focused mostly on particles much denser than the surrounding fluid (aerosols) and on light gas bubbles. It was observed that aerosol particles generally settle more rapidly than in still fluid and that their paths tend to merge into isolated long-term trajectories (hereinafter referred to as *asymptotic trajectories*) passing through the outer regions of the eddies. A plot was constructed demonstrating the nonmonotonous dependence of aerosol settling velocity on the density parameter due to the strong effects of inertia. The mechanism is the following: Inertia pushes dense particles outside the vortical cells where local fluid velocity is higher in the direction of gravity, thus determining higher effective settling velocities. The influence of vortical flows on bubbles was also investigated and it was shown that, due to negligible inertia effects, bubbles either accumulate along an isolated curve passing through the central region of each eddy, rising continuously, or else are trapped at some equilibrium point in the flow field. The tendency of both aerosol particles and bubbles to segregate preferentially in the above-mentioned flow regions was observed to produce long-term accumulation. To this, nonrandom particle distributions were attributed important effects on nonlinear concentration-dependent processes such as phytoplankton coagulation.[2]

Later studies on the settling of small, heavy particles near fixed line vortices[3] and in random two-dimensional (2D) flow,[4] confirmed the observations of Maxey[1] but indicated also that other behaviors are possible, even though less frequent. Specifically, the average settling velocity of particles in a turbulent flow can become smaller than the terminal velocity in still fluid depending on the particle properties and on the fraction of suspended particles.

To the best of our knowledge, little attention has been given to the range of particle parameters corresponding to density slightly smaller than that of the fluid. Motivation to deepen the study of this specific range comes from its relevance in the context of upper ocean and freshwater aquatic environments. Recent results from a paper by Ruiz *et al.*,[5] which refer to documented experiments, show a rise velocity of a phytoplankton species much higher than the predicted Stokes rise velocity. Ruiz *et al.*[5] attributed this discrepancy (which questions the traditional notion that turbulence diminishes phytoplankton settling in the ocean) to the higher turbulence level in the upper mixed layer of lakes and oceans: Turbulence acts like an environmental stress that can be only avoided through morphological and/or physiological adaptations. Specifically, physiological adaptations would require phytoplankton densities very close to, or a little smaller than, the density of the water: this is precisely the situation we looked at from an idealized viewpoint. We wish to remark here that a particle that is only slightly lighter than the surrounding fluid will rise but, due to the fluid which is set in motion by the particle, its trajectory may be characterized by inertia larger than that of the surrounding fluid parcels. To investigate the behavior of these particles, we decided to reproduce the experiment of Maxey,[1] focusing on the combined influence of gravity, inertia, and added mass force on the rise velocity of particles slightly lighter than the fluid (which mimics the density typical of phytoplankton cells). In this Brief Communication, we considered particles with den-

[a)]Author to whom correspondence should be addressed. Electronic mail: soldati@uniud.it

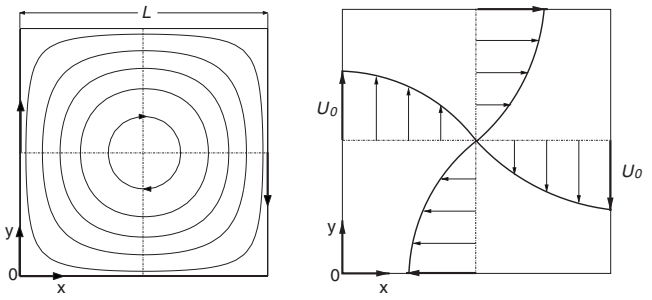

FIG. 1. (a) Streamlines and (b) velocity profiles for the periodic cellular flow field. The arrows show direction of the flow.

sity between one-half of the fluid density and the fluid density.

The incompressible cellular flow is a Taylor-Green type of vortex flow composed of a periodic array of two-dimensional eddies in square cells of size L (see Fig. 1) and can be specified by the following streamfunction:[1]

$$\psi(x,y) = \left(U_0 L/\pi\right)\sin\tilde{x}\sin\tilde{y}, \tag{1}$$

where $\tilde{x}=\pi x/L$ and $\tilde{y}=\pi y/L$. Here x and y are the coordinates aligned to the boundaries of the cells and U_0 is the fluid velocity at the cell boundaries. The scalar components of the fluid velocity vector, $\mathbf{u}$, are

$$u_x = \frac{\partial\psi}{\partial y} = U_0 \sin\tilde{x}\cos\tilde{y}, \quad u_y = -\frac{\partial\psi}{\partial x} = -U_0\cos\tilde{x}\sin\tilde{y}. \tag{2}$$

The simplified equation used to track the motion of the particles/bubbles in the steady cellular flow field has the following dimensional vector form:

$$\left(m_P + \tfrac{1}{2}m_F\right)\left(d\mathbf{V}/dt\right) = (m_P - m_F)\mathbf{g} + 6\pi a\mu(\mathbf{u}-\mathbf{V}) + m_F\mathbf{u}\cdot\nabla\mathbf{u} + \tfrac{1}{2}m_F\mathbf{V}\cdot\nabla\mathbf{u}, \tag{3}$$

where m_P is the particle mass, m_F is the mass of the displaced fluid, a is the particle radius, and μ is the fluid dynamic viscosity. Included in the right-hand side (rhs) of Eq. (3) are the buoyancy force of the fluid on the particle, the Stokes drag law, the fluid force on the particle from the stress gradients of the undisturbed flow field, and the added mass effect. The Basset history term, the aerodynamic lift force, and the Faxen corrections for the nonuniform flow field were not taken into account to reproduce exactly the simulation setting of Maxey.[1] An analysis of the order of magnitude of the forces acting on the particles, however, reveals that the added mass and the stress gradient forces are $O[(\rho_p/\rho)^{-1}]$, whereas the Basset force is $O[(\rho_p/\rho)^{-1/2}]$: for density ratios of order one, these forces become comparable. We thus remark that the pressure gradient force due to shear stress in the conveying fluid and the Basset force may produce quantitative, though not qualitative, changes to the results presented here. Similarly, the lift force can produce different particle patterns (for instance, it may push bubbles rising in a horizontal vortex to the vortex side with downward velocity) and may lead to smaller mean rise velocities.[6] Inclusion of these forces in the equation of particle motion will constitute the next step of this ongoing study.

Following Maxey,[1] the scaled form of Eq. (3) can be written as

$$d\mathbf{V}/dt = A[\mathbf{u}-\mathbf{V}+\mathbf{W}] + R\left(\mathbf{u}+\tfrac{1}{2}\mathbf{V}\right)\cdot\nabla\mathbf{u}. \tag{4}$$

The nondimensional parameters characterizing this equation are the inertia parameter, A, the particle settling velocity for still fluid, $\mathbf{W}$, and the mass (or, equivalently, density) ratio, R, which are defined as follows:

$$A = \frac{1}{St} = \frac{6\pi a\mu L}{\left(m_P + \frac{1}{2}m_F\right)U_0}, \quad \mathbf{W} = \frac{(m_P - m_F)\mathbf{g}}{6\pi a\mu U_0}, \qquad R = \frac{m_F}{m_P + \frac{1}{2}m_F} = \frac{2}{2(\rho_P/\rho_F)+1}, \tag{5}$$

where ρ_P and ρ_F are the particle density and the fluid density, respectively. Depending on the value of R, three different ranges can be identified, which correspond to different sets of physical conditions: the *aerosol range* ($\rho_P \gg \rho_F$, i.e., $0 \leqslant R \leqslant 0.4$), the *bubble limit* ($\rho_F \gg \rho_P$, i.e., $R=2$), and the *transition range* ($0.4 < R < 2$). The aerosol range and the bubble limit have been investigated in detail by Maxey.[1] In the present study, we are interested in situations where $\rho_P \leqslant \rho_F$ (particles/bubbles lighter than fluid) and $\rho_P + \rho_F/2 \geqslant \rho_F$ (fluid acceleration and added mass) become relevant perturbations to the basic aerosol problem. The combination of these two conditions corresponds to the interval $1/2 \leqslant \rho_P/\rho_F \leqslant 1$ (namely, $2/3 \leqslant R \leqslant 1$) in the transition range. The case $R=2/3$ has been considered also by Babiano *et al.*,[7] who analyzed the motion of small finite-size neutrally buoyant tracers for the purposes of targeting trajectories in an incompressible 2D flow representing a simplified chaotic Hamiltonian system.

We have investigated 38 different cases by increasing the density ratio via ρ_P. The ranges of variation for the inertia parameter and for the particle still-fluid settling velocity corresponding to the interval $2/3 \leqslant R \leqslant 1$ are $5\pi \leqslant A \leqslant 10\pi/3$ and $-0.625 \leqslant W \leqslant 0$, respectively. As in Maxey,[1] two more nondimensional parameters are introduced: the rise velocity, Q, and the inertia parameter, B, for a vapor bubble. These parameters are defined such that their value can be derived from the following equalities:[1]

$$W = \left(\frac{1}{R} - \frac{3}{2}\right)Q, \quad A = \frac{RB}{2}. \tag{6}$$

In the transition range, it is appropriate to assign fixed values to B and Q as R is varied: Here, we have chosen $B = 10\pi$ and $Q=1.25$ (Ref. 1). The components of particle velocity are computed by time integration of the following ordinary differential equations (ODEs):

$$\frac{1}{A}\frac{dV_x}{dt} + V_x = \sin\tilde{x}\cos\tilde{y} + \frac{1}{2}\frac{R}{A}(V_x\cos\tilde{x}\cos\tilde{y} - V_y\sin\tilde{x}\sin\tilde{y}) + \frac{R}{A}\sin\tilde{x}\cos\tilde{x}, \tag{7}$$

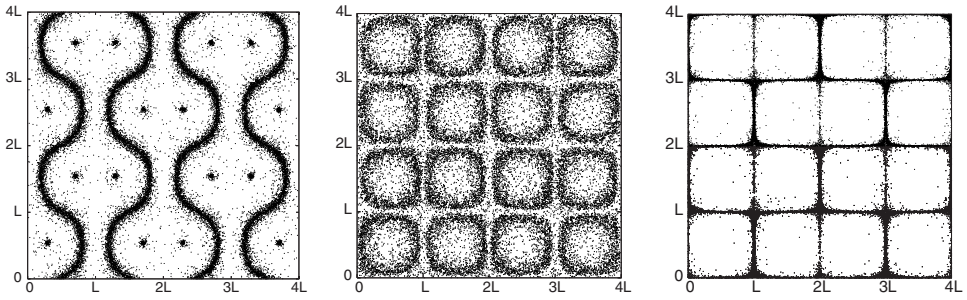

FIG. 2. Instantaneous particle position plots at time $t^*=10\,000$ for particles in the transition range: (a) $\rho_P/\rho_f=0.5$ [$R=1$, $W=-0.625$, $A/\pi=5$]; (b) $\rho_P/\rho_f=0.925$ [$R=0.675$, $W=-0.023$, $A/\pi=3.375$]; (c) $\rho_P/\rho_f=0.99$ [$R=0.671$, $W=-0.001$, $A/\pi=3.356$]. Gravity acts top down.

$$\frac{1}{A}\frac{dV_y}{dt}+V_y=-\cos\tilde{x}\sin\tilde{y}+\frac{1}{2}\frac{R}{A}(V_x\sin\tilde{x}\sin\tilde{y}-V_y\cos\tilde{x}\cos\tilde{y})+\frac{R}{A}\sin\tilde{y}\cos\tilde{y}+W.$$

All simulations were carried on until the steady-state condition for particle distribution was reached. This required a total time $t^*=tU_0/L\simeq 10^4$ per run. Note that, since the Basset history term is not included in the particle equation of motion, there is no specific initial condition on the particle velocity. In our case, the initial particle velocity has been taken to be equal to that of the fluid at the particle position. However, the motion of the particles is not sensitive to this initial condition, especially if the long-term features of the motion are investigated. Further mathematical background and a survey of the forces acting on the motion of low concentrations of finite-size, non-neutrally buoyant particles in a prescribed flow can be found in Maxey.[1]

Figure 2 shows the steady-state particle distribution for three different particle-to-fluid density ratios selected from the transition range database. For visualization purposes, only 1 particle out of 4 is plotted. From Fig. 2(a) it can be seen that particles with $\rho_P/\rho_F=0.5$ are either concentrated in the vortex center (which is a stable equilibrium point)[1,3,8] or collect along isolated accumulation curves. These curves, which eventually become neatly defined, pass through the central region of each eddy and are biased toward the upflow region of each eddy. At time t^* almost half of the particles are trapped in the vortex centers. The same sharp distribution is not observed for particles with higher density ratio. Consider, for instance, the distribution of the $\rho_P/\rho_F=0.925$ particles shown in Fig. 2(b): Even though isolated paths along the upflow region of the eddy still occur at early stages of the simulation, these particles are mainly concentrated in circular closed paths around the vortex centers at steady state. When the density ratio is further increased [$\rho_P/\rho_F=0.99$ particles, Fig. 2(c)], the only spatially coherent particle clusters are isolated curves passing preferentially through the upflow boundary of each eddy.

In Fig. 3 some sample trajectories (taken within the interval $0<t^*<10^4$) are shown for the same density ratios as in Fig. 2. The initial position of the particles is marked with a closed black circle. Being lighter than fluid, particles move upwards approaching the vortical structures from below. The inertia caused by just the particle mass is *smaller* than the inertia of the surrounding fluid. One would thus expect that particles show a tendency to be trapped within the core of the vortices. Focusing on Fig. 3(a) ($\rho_P/\rho_F=0.5$), however, we can observe two distinct behaviors: Some particles spiral in toward interior equilibrium points and never escape from their initial cell; other particles rise rapidly upwards zigzagging through the upflow region of each cell. In this latter case (which is more often observed), trajectories tend to develop the same form rather than merging. This lack of asymptotic merging is an effect of the added mass: Combining particle mass to the mass of the fluid set in motion by the particles, the overall inertia of the particle is *larger* than that of the surrounding fluid. We thus observe that particles curve outwards, away from the vortex core, driven by a mechanism somehow dual to that proposed by Wang and Maxey[9] for the case of heavy particles, which exhibit faster sedimenting velocity.

Once brought in the vortex periphery, particles can reach either its upflow side (where resuspension will be enhanced) or its downflow side (where resuspension will be reduced or inhibited), depending on the specific value of the particle-to-fluid density ratio. In the present flow, when denser $\rho_P/\rho_F=0.925$ particles are considered [see Fig. 3(b)] no inward

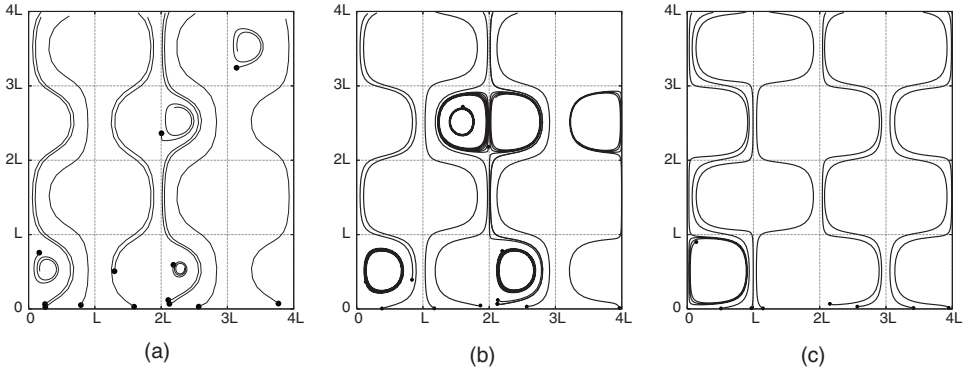

FIG. 3. Particle trajectories for particles rising through the cellular flow ($0<t^*<10\,000$): (a) $\rho_P/\rho_f=0.5$ [$R=1$, $W=-0.625$, $A/\pi=5$]; (b) $\rho_P/\rho_f=0.925$ [$R=0.675$, $W=-0.023$, $A/\pi=3.375$]; (c) $\rho_P/\rho_f=0.99$ [$R=0.671$, $W=-0.001$, $A/\pi=3.356$]. Gravity acts top down.

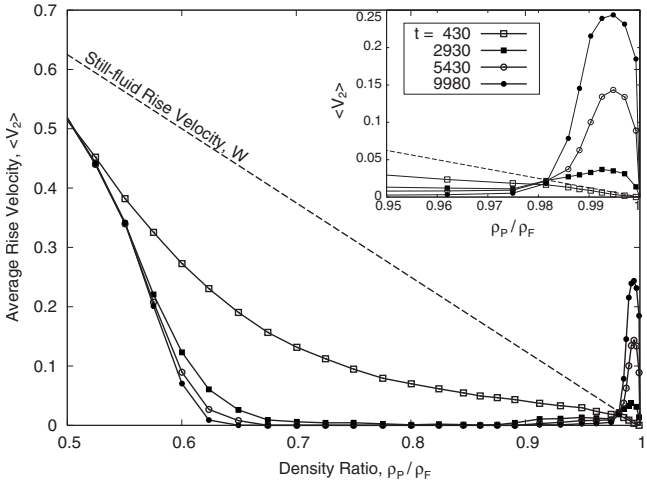

FIG. 4. Average particle rise velocity, $\langle V_2 \rangle$, against particle-to-fluid density ratio, ρ_P/ρ_F. Values of the parameters are $B/\pi=10$, $Q=1.25$.

spiraling motion is observed: Trapped particles tend to move along a well-defined closed path, which marks the position of one eddy streamline. Precisely in this case, the trajectories of rising particles indicate that accumulation occurs on the vertical cell boundaries rather than between the boundaries as found in Fig. 3(a). A further increase of particle density [see Fig. 3(c), relative to the $\rho_P/\rho_F=0.99$ particles] leads to outward spiraling motions, indicating that no equilibrium points exist: all particles will eventually rise rapidly (i.e., faster than in still fluid) through the upflow boundary of each cell. The general picture that emerges is similar to that described by Maxey for the case of light bubbles (i.e., constant particle-to-fluid density ratio) subject to different rise speeds: in the present simulations run using constant rise speed $Q=1.25$, no stable equilibrium points exist for $R \simeq 2/3$ and the particles accumulate along simple isolated curves; the effect of the stable equilibrium points becomes significant for $R \geqslant 0.7$, whereas a combination of these two responses occurs for larger values of R, with more and more particles trapped as the density ratio approaches the value $R=1$.

To provide quantitative evidence of the qualitative observations drawn in the previous figures, a plot of the average particle rise velocity, $\langle V_2 \rangle$, is shown in Fig. 4 as a function of the particle-to-fluid density ratio, ρ_P/ρ_F. The corresponding values of the still-fluid rise velocity, W, are represented by the dashed line. The $\langle V_2 \rangle$ profiles of Fig. 4 were obtained by performing an ensemble average over a sample of $5 \cdot 10^4$ particles initially distributed uniformly through the cells, and refer to four arbitrarily chosen time instants of the simulation: $t^*=430$ (solid line with open squares), $t^*=2930$ (solid line with black squares), $t^*=5430$ (solid line with open circles), and $t^*=9980$ (dashed line with black circles). We remark here that particle trajectories have not yet reached asymptotic periodicity at $t^*=430$, so the discussion is focused on the last three profiles. After an initial monotonic decrease, these profiles go through two transitions that enclose the local minimum/maximum values of $\langle V_2 \rangle$, respectively. The first transition is very smooth and produces a wide plateau (covering the range $0.675 < \rho_P/\rho_F < 0.975$) within which the values of $\langle V_2 \rangle$ are almost equal to zero. The second transition is characterized by sharp variations of $\langle V_2 \rangle$ in a very narrow range of ρ_P/ρ_F values just below unity and coincides with the local maximum, located around $\rho_P/\rho_F=0.995$: For these density values, the coupled effect of inertia and added mass segregates the rising particles into specific, fast pathlines where the local fluid velocity adds to the particle gravitational velocity. The resulting effective rise velocity is up to 40 times the absolute value of the still-fluid settling velocity for particles characterized by small differences in density [namely, by large $d\langle V_2 \rangle/d(\rho_P/\rho_F)$ gradient].

The results discussed here show the presence of a specific parameter range in which the effect of inertia combines with the effect of buoyancy giving rise to a nontrivial behavior eventually leading to surprisingly high rise velocity. The amount of this velocity increment is so remarkable that, even if the inclusion of other forces as the aerodynamic lift[6] and the Basset force can change the quantitative picture of the model, the qualitative physics may not change. Besides pinpointing a result not examined previously in this very simple scenario proposed by Maxey,[1] the value of the current findings can promote further research in the area of passive transport of nutrients in the marine environment. In particular, this Brief Communication may confirm the potential effectiveness of compensatory physiological mechanisms, such as those possibly used by phytoplankton diatoms that can adjust their density when in unlit waters,[5] to avoid sinking and sedimentation. In the frame of industrially oriented applications, these results may suggest avenues for modulation of transfer coefficients in flows with high volume fraction of microbubbles or for process control when dense gas bubbles are used. For instance, the gas density could be tuned by imposing suitable pressure levels, thus allowing optimization of the process throughput.

A.S. would like to thank Professor Detlef Lohse (University of Twente) and Professor Bruno Eckhardt (Philipps-Universität Marburg) for the stimulating discussion at the ESF Exploratory Workshop on *Challenging Lagrangian Turbulence Dynamics*, 1–4 September 2005, Castel Gandolfo, Rome.

[1] M. R. Maxey, "The motion of small spherical particles in a cellular flow field," Phys. Fluids **30**, 1915 (1987).
[2] K. D. Squires and H. Yamazaki, "Preferential concentration of marine particles in isotropic turbulence," Deep-Sea Res., Part I **42**, 1989 (1995).
[3] J. Davila and J. C. R. Hunt, "Settling of small particles near vortices and in turbulence," J. Fluid Mech. **440**, 117 (2001).
[4] C. Pasquero, A. Provenzale, and E. A. Spiegel, "Suspension and fall of heavy particles in random two-dimensional flow," Phys. Rev. Lett. **91**, 054502 (2003).
[5] J. Ruiz, D. Macias, and F. Peters, "Turbulence increases the average settling velocity of phytoplankton cells," Proc. Natl. Acad. Sci. U.S.A. **101**, 17720 (2004).
[6] I. Mazzitelli, D. Lohse, and F. Toschi, "On the relevance of the lift force in bubbly turbulence," J. Fluid Mech. **488**, 283 (2003).
[7] A. Babiano, J. H. E. Cartwright, O. Piro, and A. Provenzale, "Dynamics of a small neutrally buoyant sphere in a fluid and targeting in Hamiltonian systems," Phys. Rev. Lett. **84**, 5764 (2000).
[8] G. R. Ruetsch and E. Meiburg, "On the motion of small spherical bubbles in two-dimensional vortical flows," Phys. Fluids A **5**, 2326 (1993).
[9] L.-P. Wang and M. R. Maxey, "Settling velocity and concentration distribution of heavy particles in homogeneous isotropic turbulence," J. Fluid Mech. **256**, 27 (1993).